Journal of Applied Sciences

ISSN 1812-5654

science alert

ANSInet
an open access publisher
http://ansinet.com

Journal of Applied Sciences 9 (5): 909-916, 2009
ISSN 1812-5654

The Performance of Laterally Loaded Single Pile Embedded in Cohesionless Soil with Different Water Level Elevation

[1]M.R. Taha, [1]Jasim M. Abbas, [2]Qassun S. Mohammed Shafiqu and [1]Zamri H. Chik
[1]Department of Civil and Structural Engineering, Universiti Kebangsaan Malaysia, Selangor, Malaysia
[2]Department of Civil Engineering, Nahrain University, Iraq

Abstract: A three-dimensional finite element simulation is presented in this study to investigate the lateral pile response for single vertical pile embedded in cohesionless soil. Four water table cases we simulated, i.e., dry soil condition, water table in the base and middle of the pile length and fully saturated soil. Linear elastic model of pile is used for modeling the pile material while Mohr-Coulomb model is used to simulate the surrounding soil. The pile-soil interaction are composed of 16-node interface elements. It was found that the water table elevation influence on the behavior of laterally loaded pile. As expected the case of dry soil condition gives more resistance than other three soil cases.

Key words: Laterally loaded pile, pile-soil interaction, 3D FEM, soil stresses, pile stresses

INTRODUCTION

In general, pile foundation is used when heavy engineering buildings structures have to be transfer superstructure loads to the deep strong stratum. Most piles are generally subjected to lateral load as well as vertical load. The design of pile under lateral loading will be dependent on the satisfying a limiting lateral-deflection requirement that may result in the specification of allowable lateral loads which much less than ultimate lateral capacity of the pile. Accurate ground water level information is needed for the estimation of soil densities, determination of effective soil pressures and preparation of effective soil pressure diagrams. This information is vital for performing foundation design.

Current method of analysis available to study single pile and pile groups depends on the direction of loading, i.e., pure vertical or pure horizontal. For pure lateral loading on piles, there are three methods of analyses which can be categorized into (Poulos and Davis, 1980): (1) beam on elastic foundation method-subgrade reaction; (2) elastic continuum method and (3) the finite element method. Trochanis *et al*. (1991), Yang and Jeremiae (2005), Johnson (2006) and Tahghighi and Kongai (2007) used the finite element method to numerically study piles response to pure lateral loads.

In most practical cases, the piles are subjected to both vertical and horizontal loads. The influence of the vertical load intensity on lateral response of the piles was studied by Karthigeyan *et al*. (2006, 2007) using a general three-dimensional finite element analysis for cohesion and cohesionless soil. According this study, the response of pile in both soil type under lateral loads in influenced by the response of vertical loads.

This study reports the result of preliminary three-dimensional finite element analysis on laterally loaded pile embedded in cohesionless soil, considering it considers load intensity and water table elevation variation of the foundation soils in consideration of the lateral pile deformation, lateral soil pressure, lateral shear stresses and induced stresses on piles.

FINITE ELEMENT MODELS AND MESH GENERATION

Finite element analysis were performed using the software PLAXIS 3D FOUNDATION version 1.1. In the finite element method a continuum is divided into a number of (volume) elements. Each element consists of a number of nodes. Each node has a number of degrees of freedom that correspond to discrete values of the unknowns in the boundary value problem to be solved.

In order to perform the finite element calculations, the geometry has to be divided into elements. A composition of finite elements is called finite element mesh. The basic soil elements of a 3D finite element mesh are represented by the 15-node wedge elements as shown in Fig. 1a. These elements are generated from the 6-node triangular

Corresponding Author: Jasim M. Abbas, Department of Civil and Structural Engineering, Faculty of Engineering and Built Environment, Universiti Kebangsaan Malaysia, Selangor D H, 43600 Bangi, Malaysia Tel: 0060176384641

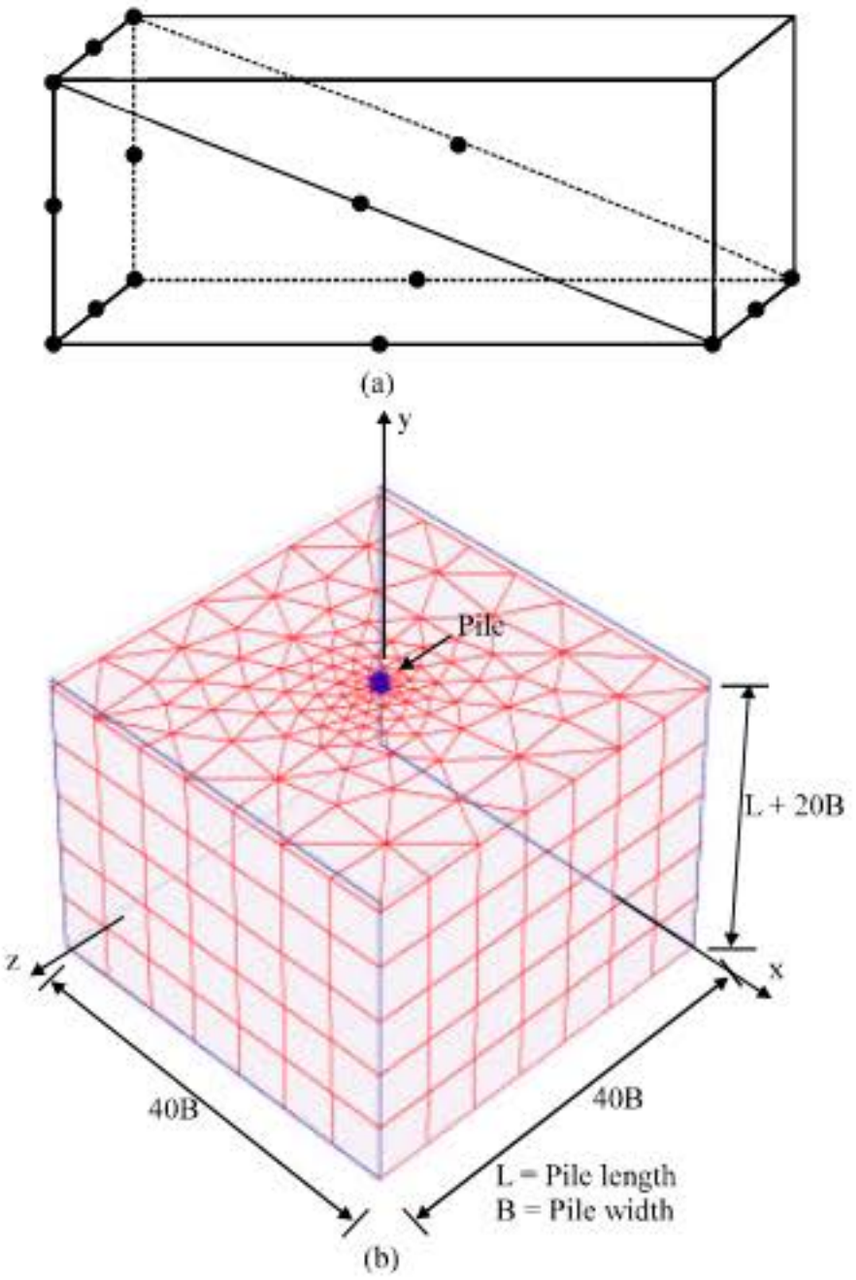

Fig. 1: 3D finite element mesh for soil mass and location of pile, (a) 15-node wedge element and (b) 3DFE mesh

elements. The 15-node wedge element is composed of 6-node triangles in horizontal direction and 8-node quadrilaterals in vertical direction. According to Karthigeyan (2006, 2007), the soil mass dimension depends on the pile diameter and length. The width of soil mass is taken as 40B, in which, B is the pile diameter or pile width. The soil mass affection the pile response diminishes when the width is greater than 40B. The height of soil mass is L+20B, in which, L is the length of pile as shown in Fig. 1b.

CONSTITUTIVE MODELS

Linear-elastic model: Hooke's law is the main constitutive law in the theory of elasticity as shown in Fig. 2. It provides the relationship between the stresses and strains at all points within the body and it is used here for modeling the stress-strain relationship of the pile material. The model involves two elastic stiffness parameters, namely Young's modulus, E and Poisson's ratio, v. It is primarily used for modeling of stiff structural member for example piles in the soil (Johnson *et al*., 2006).

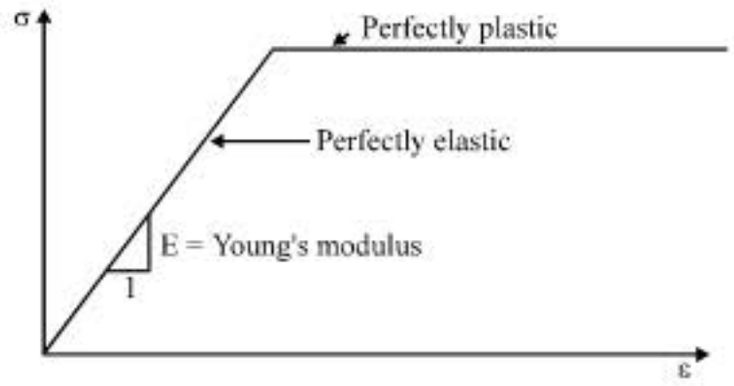

Fig. 2: Stress-strain curve

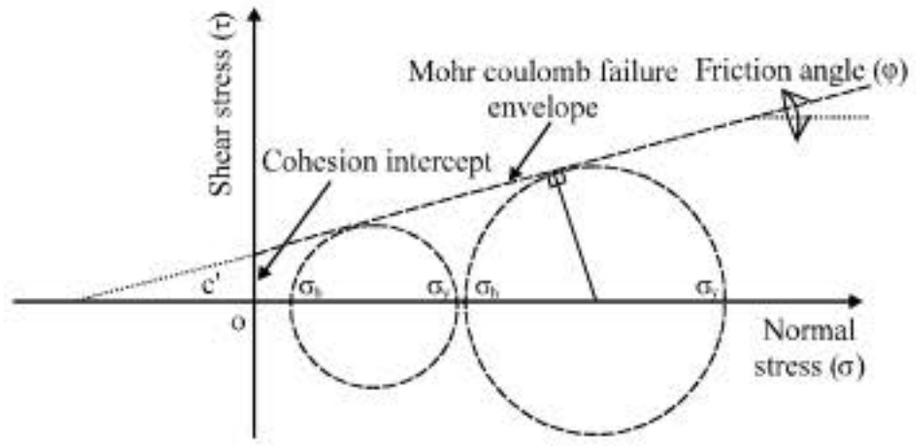

Fig. 3: Mohr coulomb's failure surface

Mohr-coulomb model: The Mohr-coulomb model is used in this study to compute realistic bearing capacities and collapse loads of footings or foundation soils. As well as other applications in which the failure behavior of the soil plays a dominant role. This elasto-plastic model is based mainly on two soil parameters that are known in most practical situations. These parameters are the effective cohesion intercept, c' and the friction angle, ϕ'. In addition three parameters namely Young's modulus, E, Poisson's ratio, v and the dilatancy angle, ψ are needed to calculate the complete σ-ϵ behavior. Mohr coulomb's failure surface criteria are shown in Fig. 3. According to Johnson (2006), the failure envelope only depend on the principal stresses (σ_1, σ_3) and is independent of the intermediate principle stress (σ_2). When mapped in three-dimensional stress space, Mohr-coulomb criteria resolved into an irregular hexagonal pyramid. This pyramid forms the failure/yield envelope, which in turn governs how soil will behave. The material behaves elastically if the stress point lies within the failure envelope. However, if the stress reaches the yield surface the material will undergo plastic deformation. In the Mohr-coulomb model used herein, it is assumed that the soil has a linear elastic relation until failure.

The usual definition of the equation of Mohr-coulomb surface is (Potts and Zdravkovic, 1999):

$$F = \frac{\sigma_1' + \sigma_3'}{2}\sin\phi' - \frac{\sigma_1' + \sigma_3'}{2} - c'\cos\phi' \qquad (1)$$

Which, when rewritten in terms of invariants and Lode angle θ becomes:

$$F = \frac{1}{3} I_1 \sin\phi' + \sqrt{j_2}\left(\cos\theta - \frac{\sin\theta \sin\phi'}{\sqrt{3}}\right) - c' \cos\phi' \quad (2)$$

Where:

$$I_1 = \sigma_x' + \sigma_y' + \sigma_z' \quad (3)$$

and

$$J_2 = \frac{1}{6}\left\{(\sigma_x' + \sigma_y')^2 + (\sigma_y' + \sigma_z')^2 + (\sigma_z' + \sigma_x')^2\right\} + \tau_{xy}^2 + \tau_{yz}^2 + \tau_{xy}^2 \quad (4)$$

Interface element: The response of a soil-structure system subjected to static and dynamic loadings can be influenced significantly by the characteristics of the contacts between the structure and the soil. Often, in the soil-soil and soil-structure interaction complete bonding in the contact plane was assumed to perform the design analysis. Although that assumption simplifies the analytical procedure, it underestimates the actual response as no relative motions are included. Thus, for a realistic simulation of these problems it may be appropriate to incorporate such motions using special finite elements, like the interface elements.

Interfaces are modeled as 16-node interface elements. Interface elements consist of eight pairs of nodes, compatible with the 8-noded quadrilateral side of a soil element (Fig. 4). Along degenerated soil elements, interface elements are composed of 6-node pairs, compatible with the triangular side of the degenerated soil element. Each interface has a virtual thickness assigned to it which is an imaginary dimension used to obtain the stiffness properties of the interface. The virtual thickness is defined as the virtual thickness factor times the average element size. The average element size is determined by the global coarseness setting for the 2D mesh generation. The default value of the virtual thickness factor that is used in this study is 0.1. The stiffness matrix for quadrilateral interface elements is obtained by means of Gaussian integration using 3×3 integration points. The position of these integration points (or stress points) is chosen such that the numerical integration is exact for linear stress distributions. The 8-node quadrilateral elements provide a second-order interpolation of displacements. Quadrilateral elements have two local coordinates (ξ and η).

Verification problem: Verification example is worked out to compare results obtained by finite element analysis to those obtained from experimental study. The case study deals with lateral load in which the deflection response of bored piles in cemented sand were examined by field test on single pile under lateral load (Ismael, 1998). All piles were 0.3 m in diameter and had a length of 3 or 5 m. The site of this load test was in Kuwait. The surface soil to depth of 3.5 m was characterized as having both components of shear strength, both effective parameters. The soil profile consists of a medium dense cemented silty sand layer to a depth 3 m. This is underlain by medium dense to very dense silty sand with cemented lumps to the bottom of the borehole. The geotechnical properties of the soil layers are shown in Table 1. Ground water was not encountered within the depth of the borehole.

The comparison between the finite element results and field test data is shown in Fig. 5. Comparable data

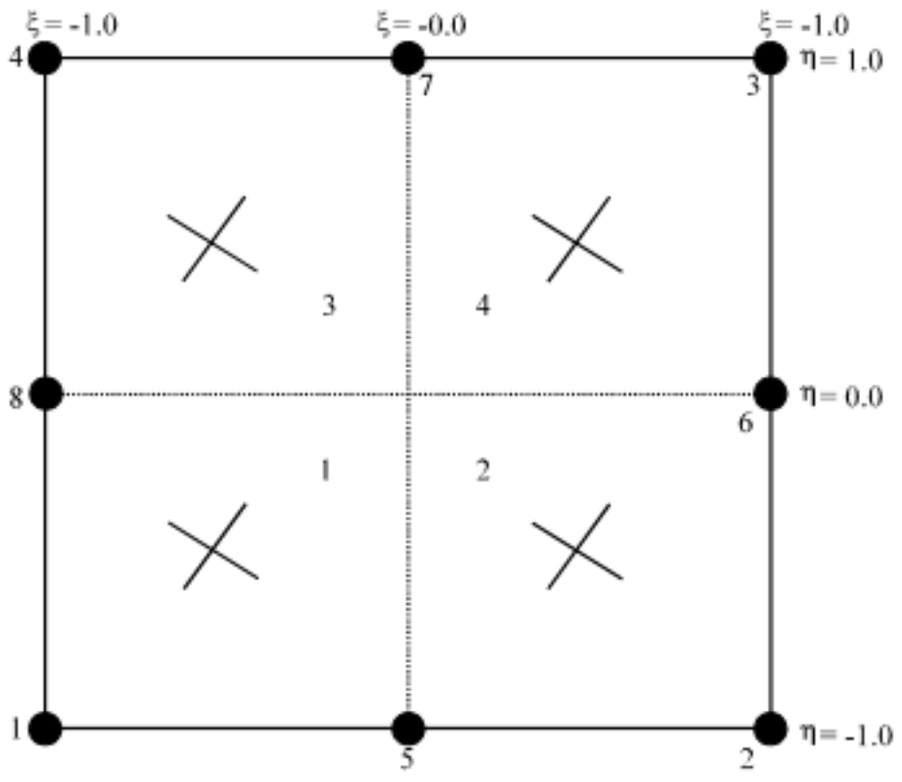

Fig. 4: Local numbering and positioning of nodes (●) and integration points (x) of an 8-node quadrilateral element

Table 1: Geotechnical properties of the soil layers

Parameters	Name	Medium dense cemented silty sand layer	Medium dense to very dense silty sand with cemented lumps	Pile	Unit
Unsaturated soil weight	γ_{unsat}	18	19	25	kN m^{-3}
Saturated soil weight	γ_{sat}	18	19	-	kN m^{-3}
Young's modulus	E	1.300 E+04	1.300 E+04	2 E+09	kPa
Poisson's ratio	v	0.3	0.3	0.15	-
Cohesion intercept	c'	20	1	-	kPa
Friction angle	ϕ'	35	45	-	-

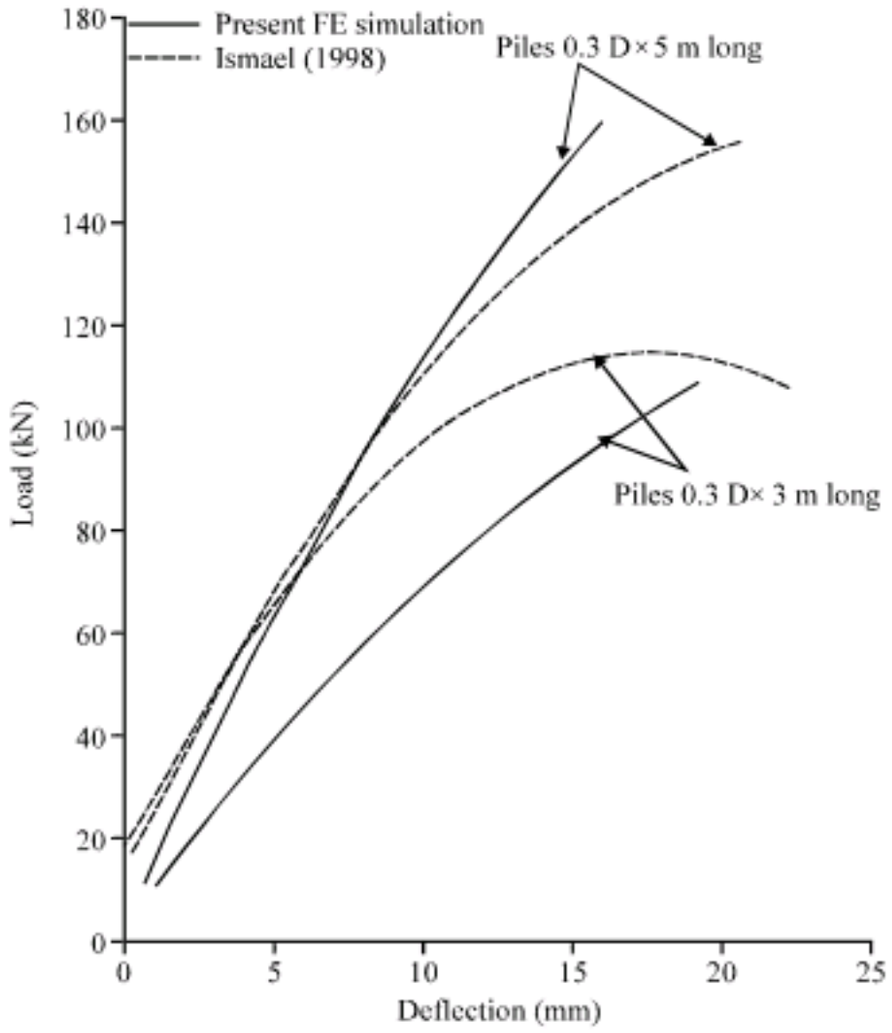

Fig. 5: Comparison of finite element results with field test data from Ismael (1998)

were obtained between the experimental results. The numerical simulation is reasonably accurate for the problem of laterally loaded piles and pile-soil interaction over a wide range of deformation for 3 and 5 m piles long. It can also be observed that the 5 m pile length has a higher lateral resistance compared to the 3 m pile.

RESULTS AND DISCUSSION

The lateral soil resistance is one of the most important factors that directly effect on the pile response under such loads. This performance depends on the interaction between pile material and the surrounding soil. This study includes: (i) effect of changing the water table elevation possibly due to the weather and other environmental conditions on the behavior of pure laterally loaded pile and (ii) effect of lateral load intensity on the behavior of pile under pure lateral load. Two load intensities were studied, i.e., 50 and 250 kN.

Parametric studies: The analysis consists of modeling of single short pile using linear-elastic model with 15-node wedge elements. The cross-section of the pile is circular with a diameter of 1.2 m. The pile was loaded under pure lateral load in two stages. Circular pile was used to simulate the behavior of piles under lateral loads. These piles were embedded into a sandy soil layer. The tested pile, dimensions and soil properties are summarized in Table 2.

Table 2: Pile and soil properties

Pile details	Values	Soil details	Values
Size	1200 mm D	Friction angle (f_0)	30
Length	10 m	Dilation angle (ψ_0)	0-10
Type of pile	Concrete	Unit weight (γ)	18 kN m^{-3}
Grade of concrete	M 25	Young's modulus (Es)	20 MPa
Young's modulus Ep	25000 MPa	Earth pressure (k_0)	0.5
Poisson's ratio (vs)	0.15	Poisson's ratio (v)	0.3

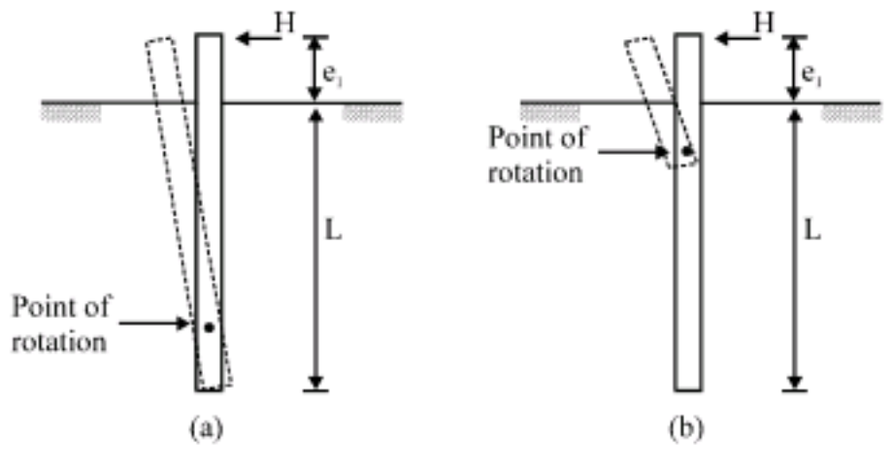

Fig. 6: Failure modes of vertical piles (a) short pile and (b) long pile under lateral loads (Poulos and Davis, 1980)

Four soil conditions were studied with respect to the ground water table. First of all, dry soil condition was analyzed. Then the water table was set at the base of the pile and the middle length of the pile. Finally the whole soil was considered fully saturated.

Assessment of lateral deflection and lateral soil pressure: In the design of pile subjected to lateral load, the ultimate lateral resistance of pile is required to satisfied two criteria (Patra and Pise, 2001; Poulos and Davis, 1980), (i) normal deflection at working loads should be within the permissible limit ; and (ii) pile should be safe against ultimate failure.

The upper part of pile is the most critical part in the case of laterally loaded pile (Poulos and Davis, 1980) because of its greater deflection and its ability to carry higher lateral loads than the lower part as shown in Fig. 6. The short pile theory assumed that the point of rotation is near the base of pile which means that soil failure will take place but no fracture occurs as in the case of long pile as shown in Fig. 6a and b, respectively. According to Zhang *et al*. (2005) the overall soil resistance occurred in the soil beneath the piled foundation is the summation of front soil pressure and side shearing stress. The lateral soil resistance distributed uniformly between the two sides of pile in opposite direction to the lateral load with greatest value occurred at the middle on pile, while the maximum shear stress occurred in the pile side as shown in Fig. 7.

Figure 8 shows the lateral deformation along the length of pile with different loadings and water table elevation. It was found that for both magnitudes of loadings (50 and 250 kN) the lateral deformation of pile in

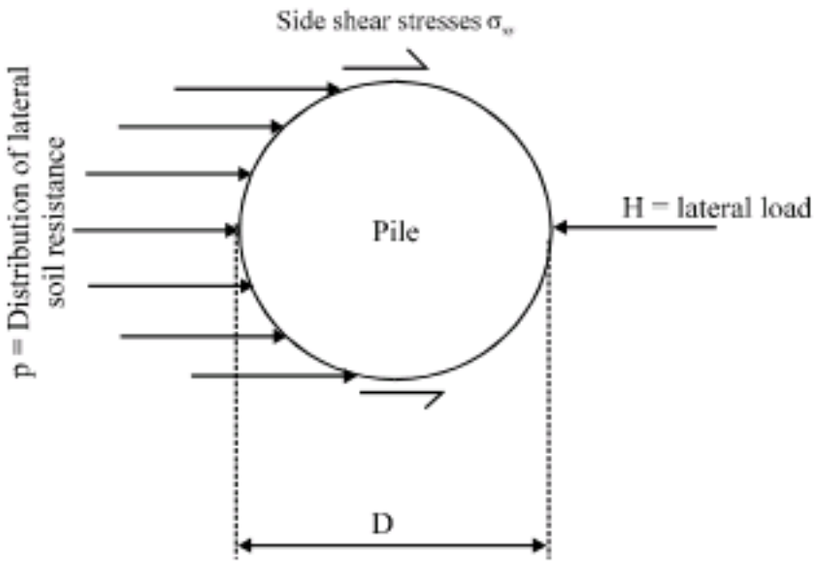

Fig. 7: Distribution of earth pressure subjected to lateral load (Zhang *et al*., 2005)

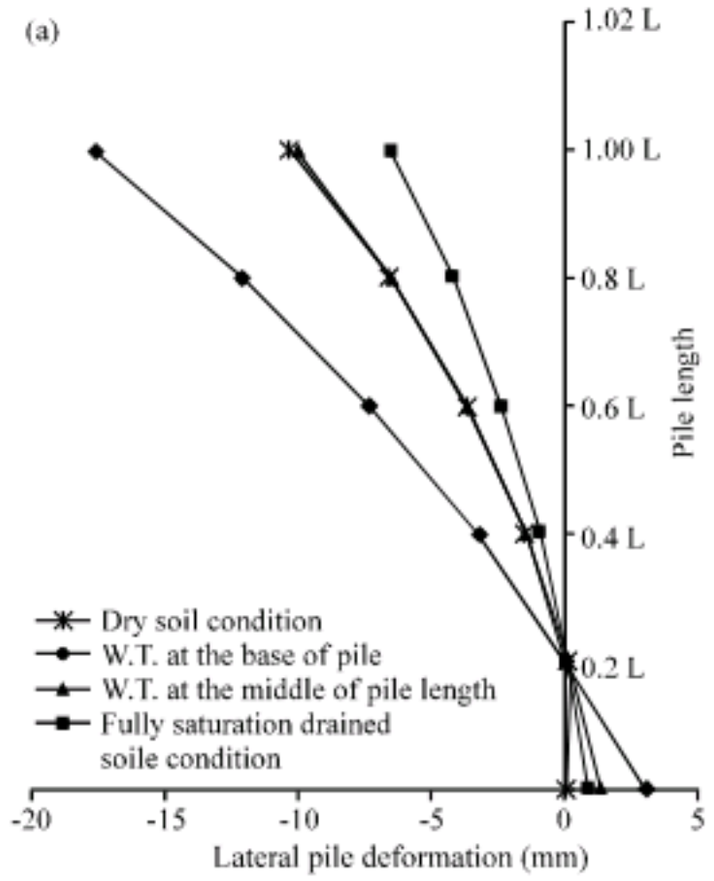

Fig. 8: Lateral pile deformation, (a) lateral load = 250 kN, (b) lateral load = 50 kN

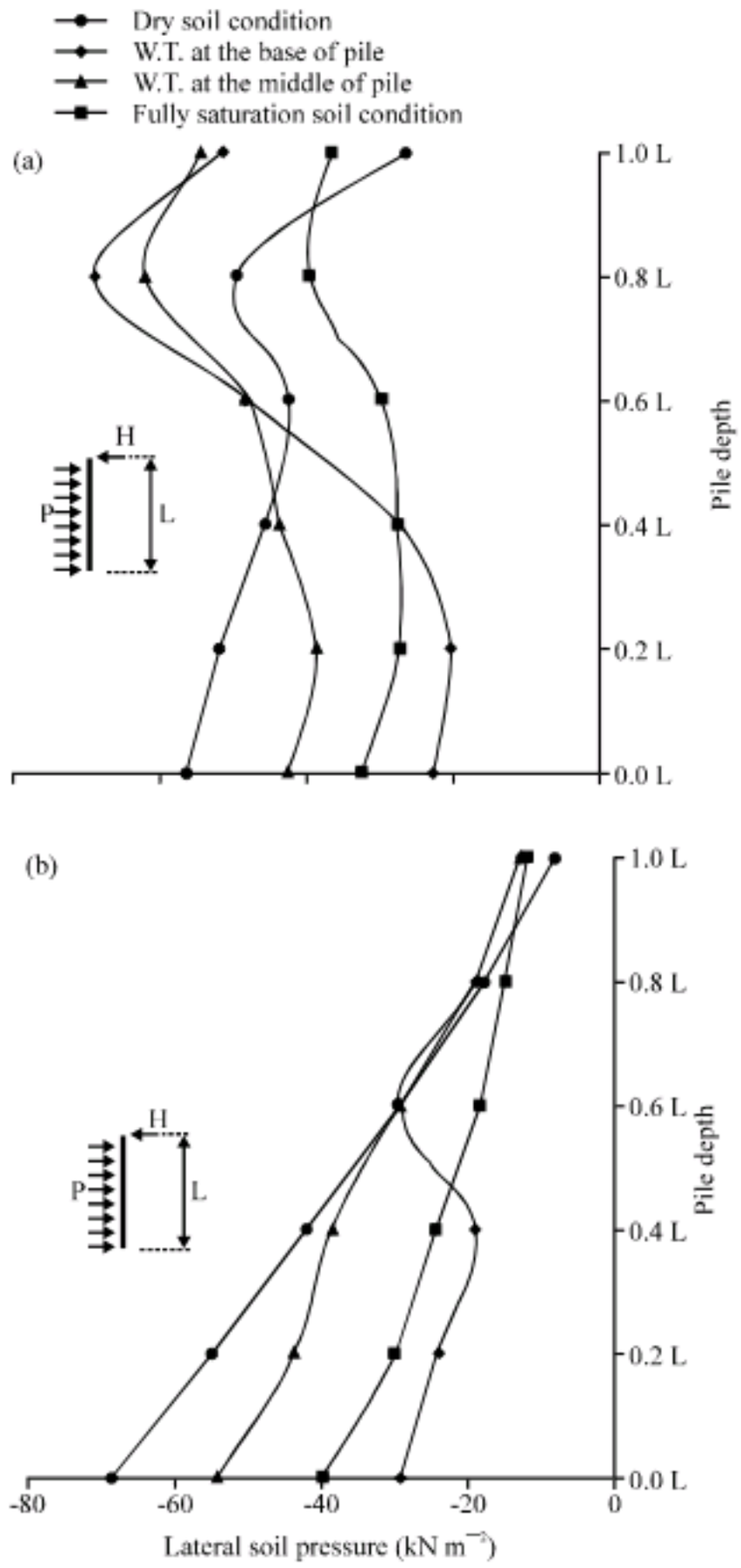

Fig. 9: Distribution of front soil pressure along pile length (depth), (a) lateral load = 250 kN, (b) lateral load = 50 kN

the case of dry soil and W.T. in the middle of pile were almost the same. Also when the water table elevation was at the base of the pile, largest lateral deformation occurred. From Fig. 8 it can be predicted that the lateral deformation shape is not straight line especially in the upper part between e = 1 L and e = 0.6 L. This means that the pile has point of fracture at this critical part of pile. In the lower part of pile one can see the point of rotation at 0.2 L, which means the negative lateral deformation occurred.

It is important to study the lateral soil pressure along pile length in order to understand which part of the pile carry larger soil pressure that may cause pile collapse. Figure 9 shows the distribution of the lateral soil pressure

with depth of pile under different water table elevation. In the case of small lateral loading (50 kN) it was predicted that the pressures increased with depth in the four soil conditions with a maximum value of 68.5 kN m^{-2} at the base under dry soil condition. In the case when the water table is at the base of pile it was noticed that at depth 0.6 L the lateral soil pressure started to decrease and reached the minimum value at about 0.4 L. However, when the lateral load was increased to 250 kN, the soil performance changed. The figure show that maximum soil pressure is concentrated at 0.8 L and thus this point can be considered as the critical point in the design as well as the fracture point. This is in line with those recommended by Poulos and Davis (1980).

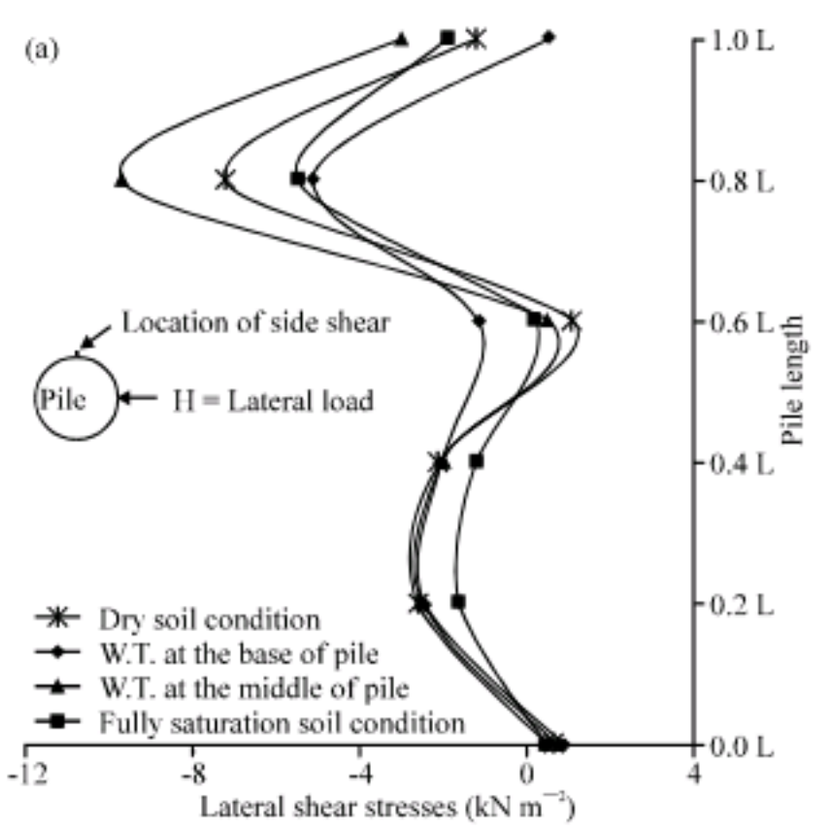

Fig. 10: Distribution of front soil pressure along pile length (depth), (a) lateral load = 250 kN, (b) lateral load = 50 kN

The lateral soil shear resistance is shown in Fig. 10. The value of lateral shear soil resistance is small compared with lateral soil pressure. Therefore the lateral response of pile depends mainly on the front soil pressure and less for side shear. The maximum value occurred at e = 0.8L and reduced to very low near the base of pile for both loading intensity (50 and 250 kN). Also the reduction in the side shear can be seen at e = 0.6L and could change to negative at this depth when the lateral load of 250 kN was applied. This means that at this depth the side shear resistance is neglected for calculation of the total soil resistance.

Assessment of internal pile stresses: The pile can be improved as a structural column under lateral load or at least as cantilever beams. By considering the effect of surrounding soil on the behavior of this structural member. Due to the load, the pile showed two zones of stresses; the first is compression and it occurred always in the opposite side of applied load and the second zone represent the tension part of the member and is always on the same side of the applied load as shown in Fig. 11. The tension zone is very critical as the cracks normal occur in this part.

Figure 12 shows the compression and tension stresses that developed in the pile under pure lateral load. In the case of a low loading value (50 kN) no different found in the values of compression and tension stresses. For a high loading (250 kN) one can observe the difference in values especially for fully saturated soil condition. This means that the pile in this soil condition (saturated soil) is less resistant than that in other soil conditions. The greatest value for both compression and tension stresses occurred in the zone between e = 0.6 L and 0.8 L in the case of low loading. However the maximum values in the case of high loading occurred at e = 0.6 L. From the figure it can be seen that the tension stresses change in sign between e = 0 and 0.2 L for low loading as the pile rotate at this point. For higher pile loading the change in sign appears very clearly at the pile base.

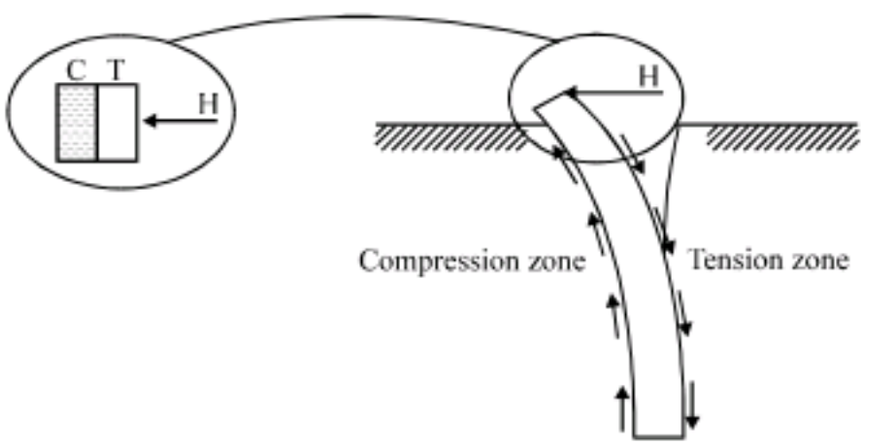

Fig. 11: Compression and tension zones of a laterally loaded pile

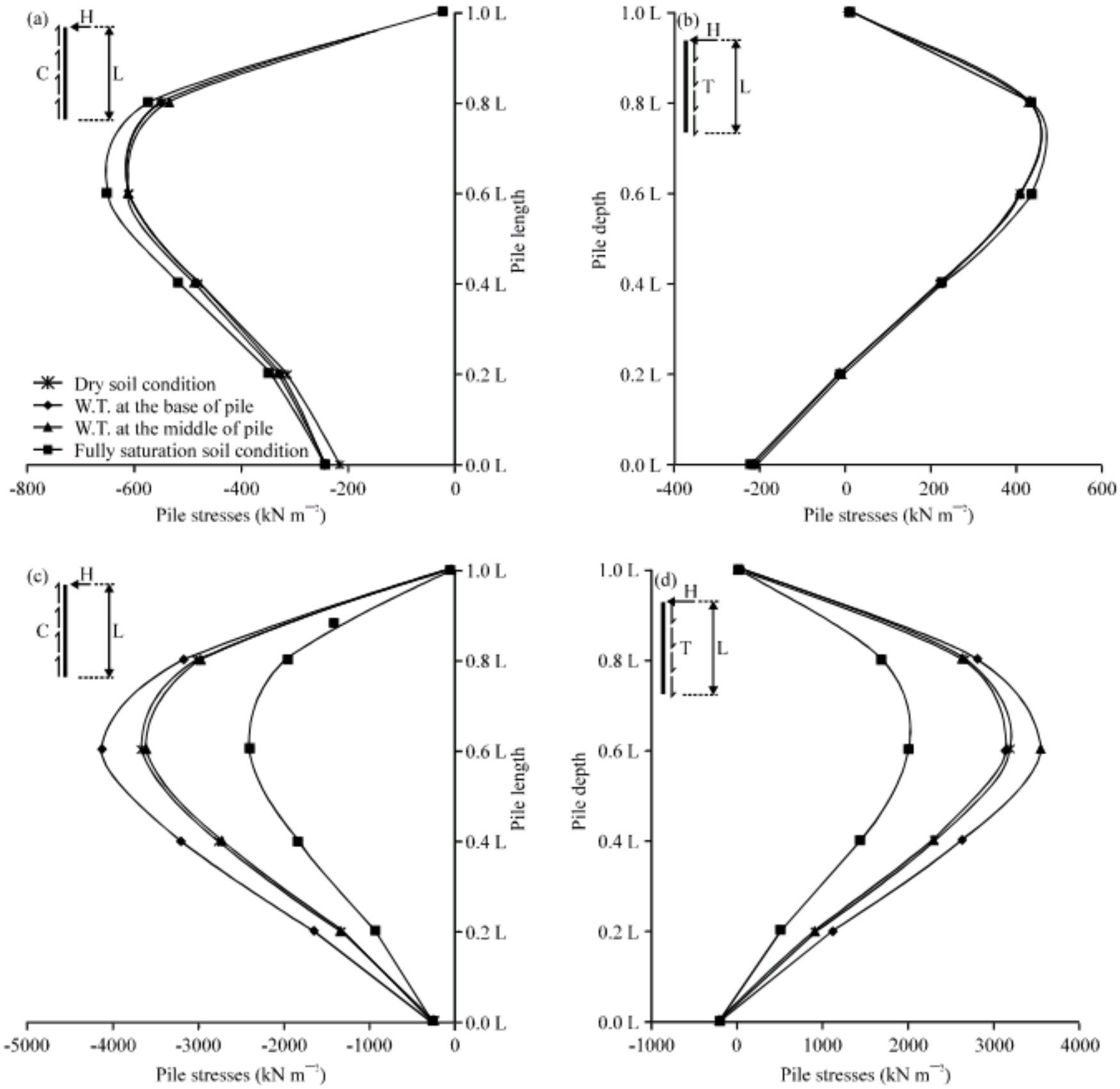

Fig. 12: Pile structural stresses, (a, b) Effect of low loading value (H = 50 kN) on compression and tension and (c, d) Effect of high loading value (H = 250 kN) on compression and tension

CONCLUSION

A three-dimensional finite element analysis have been used for the assessment of the behavior of laterally loaded pile. From this investigation, the following conclusions can be drawn:

- The water table elevation affected the behavior of laterally loaded pile
- The response of the pile in cohesionless soil under lateral load is influenced by the magnitude of horizontal load
- The greatest magnitude of lateral soil pressure occurred at e = 0.8 (near to surface) and this section is more critical than other parts of pile
- Lateral shear soil resistance is small comparing with lateral soil pressure (between 10-13%) which means that the soil resistance depends mainly on the front soil pressure
- Pile structural stresses is influenced by the magnitude of load and water table elevation

REFERENCES

Ismael, N.F., 1998. Lateral loading tests on bored piles in cemented sands. Proceedings of the 3rd International Geotechnical Seminar on Deep Foundation on Bored and Auger Piles, October 19-21, Ghent, Belgium, pp: 137-144.

Johnson, K., P. Lemcke, W. Karunasena and N. Sivakugan, 2006. Modelling the load-deformation response of deep foundation under oblique load. Environ. Modell. Software, 21: 1375-1380.

Karthigeyan, S., V.V.G.S.T. Ramakrishna and K. Rajagopal, 2006. Influence of vertical load on the lateral response of piles in sand. J. Comput. Geotechnol., 33: 121-131.

Karthigeyan, S., V.V.G.S.T. Ramakrishna and K. Rajagopal, 2007. Numerical investigation of the effect of vertical load on the lateral response of piles. J. Geotech. Geoenvir. Eng. ASCE., 133: 512-521.

Patra, N.R. and P.J. Pise, 2001. Ultimate lateral resistance of pile groups in sand. J. Geotech. Geoenviron. Eng. ASCE., 127: 481-487.

Potts, D.M. and L. Zdravkovic, 1999. Finite Element Analysis in Geotechnical Engineering: Theory. 1st Edn., Thomas Telford Ltd., Heron Quay, London, ISBN: 0 7277 2753 2.

Poulos, H.G. and E.H. Davis, 1980. Pile Foundation Analysis and Design. 1st Edn., John Wiley and Sons, Inc., United States, ISBN: 0-471-02084-2.

Tahghighi, H. and K. Konagai, 2007. Numerical analysis of nonlinear soil-pile group interaction under lateral loads. Soil Dynamic Earthquake Eng., 27: 463-474.

Trochanis, A.M., J. Bielak and P. Christiano, 1991. Three-dimensional nonlinear study of piles. J. Geotech. Eng., 117: 429-447.

Yang, Z. and B. Jeremiae, 2005. Study of soil layering effects on lateral Loading behavior of piles. J. Geotech. Geoenvir. Eng. ASCE., 131: 762-770.

Zhang, L., F. Silva and R. Grismala, 2005. Ultimate lateral resistance to pile in cohesionless soils. J. Geotech. Geoenvir. Eng. ASCE., 131: 78-83.